Open Access Full Text Article

ORIGINAL RESEARCH

Doxorubicin and Edelfosine Combo-Loaded Lipid–Polymer Hybrid Nanoparticles for Synergistic Anticancer Effect Against Drug-Resistant Osteosarcoma

Ping Yang
Lian Zhang
Tian Wang
Qi Liu
Jing Wang
Yaling Wang
Zhiquan Tu
Feng Lin

Department of Oncology, The Eighth People's Hospital of Shanghai, Shanghai 200233, People's Republic of China

Introduction: The failure of chemotherapy in osteosarcoma results in drug resistance and acute side effects in the body.

Methods: In this study, we have prepared a novel folate receptor-targeted doxorubicin (DOX) and edelfosine (EDL)-loaded lipid–polymer hybrid nanoparticle (DE-FPLN) to enhance the anticancer efficacy in osteosarcoma. The nanoparticles were thoroughly characterized for in vitro biological assays followed by detailed antitumor efficacy analysis and toxicity analysis in a xenograft model.

Results: The dual drug-loaded nanoparticles showed a nanosized morphology and physiological stability. The targeted nanoparticles showed enhanced cellular internalization and subcellular distribution in MG63 cancer cells compared to that of non-targeted nanoparticles. Among many ratios of DOX and EDL, 1:1 ratiometric combinations of drugs were observed to be highly synergistic in killing the cancer cells. MTT assay and caspase-3/7 activity assay clearly showed the superior anticancer efficacy of DE-FPLN formulations in inducing the cancer cell death. In vitro results indicate that the co-administration of two drugs in a folic acid-targeted nanoparticle could potentially induce the apoptosis and cell death. In vivo results displayed the potency of tumor cell killing and significant suppression of tumor growth without any detectable side effects.

Conclusion: The lipid–polymer hybrid nanocarriers with multiple properties of high drug loading, sequential and ratiometric drug release, improved physiological stability, prolonged blood circulation, and tumor-specific targeting are promising for the delivery of multiple drugs in the treatment of osteosarcoma.

Keywords: osteosarcoma, doxorubicin, edelfosine, nanoparticles, apoptosis, combination chemotherapy

Introduction

Osteosarcoma is one of the common forms of bone cancer, accounting for 60% of all bone cancer cases.[1] Osteosarcoma mainly affects children and adults of age 10–18 years or within the first 2 decades of their life. It mainly originates from mesenchymal cells and largely presents in large bones such as the femur or tibia.[2] Later on, primary osteo cells spread to the lungs, making it difficult to treat. The recent development in technology and diagnosis did not improve the 5-yearsurvival rate which is still ~65%, making it a big cause of concern. Current treatment

Correspondence: Feng Lin
Email fenglinxx1972@yahoo.com

8055

options include surgery followed by chemotherapy. Several high doses of anticancer drugs such as doxorubicin, cisplatin, and ifosfamide were used to treat osteosarcoma; however, none led to satisfactory cure or treatment.[3,4] The failure of chemotherapy mainly arises from drug resistance and acute side effects of a high dose of anticancer drugs.[5] Therefore, a novel strategy needs to be developed to improve the survival rate and therapeutic efficacy in osteosarcoma.

Combination of chemotherapeutic drugs is adapted as a standard therapy in the clinic compared to single drug administration. The combination of anticancer drugs acts in multiple pathways and effectively kills the cancer cells compared to that of single drugs, which often result in failure or lead to drug resistance. In this regard, doxorubicin (DOX) is an anthracycline analog widely used for the treatment of osteosarcoma as well as multiple other cancers such as breast cancer or leukemia.[6] Despite being one of the effective drugs available on the market, its anticancer efficiency is often hampered by the development of multidrug resistance (MDR) that led to the progression of recurrence of cancer tissues. The main reason behind MDR is believed to be ATP-binding cassette transporters such as p-gp that pumps the drug out of the cancer cells.[7] Moreover, anthracyclines are substrates for p-gp and therefore responsible for MDR and failure in the chemotherapy process, and hinder its application at the clinical level.[8] In order to reverse these limitations, combination of a second agent was considered an appropriate strategy. Edelfosine (EDL) has been reported to exhibit synergistic therapeutic effect in osteosarcoma and has been reported to significantly decrease the dose of DOX administration.[9] The alkyl-lysophospholipid has been shown to be efficacious in many cancer cells. The mechanism of action involved with EDL involves binding the lipid rafts of the plasma membrane inducing extrinsic apoptosis pathways.[10,11] Also, it induces apoptosis via mitochondria and the endoplasmic reticulum.[12,13] Two different therapeutic targets of the nucleus and the membrane are expected to improve the therapeutic efficacy and minimize the adverse effects.[14] However, when administered in the free form, several drawbacks such as poor bioavailability and rapid clearance from the systemic circulations are reported.

Lipid–polymer hybrid nanoparticles (LPN) have recently emerged as a potent alternative to lipid or polymer nanoparticles separately.[15] LPN are typically polymeric nanoparticles embedded by biocompatible lipid layers. Both drugs (DOX and EDL) are stably loaded in the hydrophobic PLGA and lipid structures.[16] The protective lipid layers effectively decrease the release of encapsulated drugs in systemic circulation and thereby reduce the side effects to normal cells.[17] The presence of polyethylene glycol (PEG) on the lipid shell improves the stability of particles and prevents the absorption of serum protein, and thereby prolongs its systemic circulation.[18,19] These properties allow the accumulation of nanoparticles in the tumor tissues via a well-known enhanced permeability and retention (EPR) effect. In order to further increase the drug accumulation, targeting of nanoparticles to the tumor tissues would be beneficial.[20] In this regard, folate receptors (FR) which are overexpressed in the cancer cells bind specifically to the folic acid molecules.[21] The folate receptors are less expressed in the normal cells while overexpressed in the cancer cells and bind to folic acids in the nanoparticles.[22]

The main aim of the present study was to prepare DOX and EDL-loaded lipid–polymer hybrid nanoparticles in order to increase the therapeutic efficacy in osteosarcoma. Anthracyclins such as DOX form complexes with DNA and inhibit topo-isomerase II, leading to cancer cell death. However, DOX is a substrate of ATP-binding cassette (ABC) transporters which efflux the drug outside the cancer cells and limit its cytotoxicity. Besides, DOX has been reported to cause severe systemic side effects to the vital organs.[23,24] Therefore, the present study aimed to increase the anticancer efficacy of DOX while minimizing the adverse effects to the normal organs. In this regard, EDL has been selected as an appropriate drug that does not target the DNA but rather binds to membrane lipid rafts, induces the damage of transmembrane proteins, and initiates the numerous apoptosis signaling pathways. Therefore, the present study attempted the combination of DOX and EDL as a targeted co-delivery system for synergistic therapeutic effect. The dual drugs were loaded in the LPN and characterized for a wide range of in vitro and in vivo animal studies. The anticancer efficacy was tested in MG63 cancer cell-based xenograft tumor models. Recently, González-Fernández et al have reported the combination of DOX and EDL and demonstrated synergistic effect in osteosarcoma cells; however, the study was limited to in vitro conditions.[25] In the present study, we have explored a detailed in vivo therapeutic efficacy in xenograft model and established the toxicity profile of free drugs and the nanoparticle-based combination.

Materials and Methods
Materials
DOX (>99%) was purchased from Beijing Zhongshuo Pharmaceutical Technology Development. Poly(lactic-co-glycolic acid) (PLGA, 50/50) and EDL were purchased from Sigma-Aldrich (China). 1,2-Distearoyl-sn-glycero-3-phosphoethanolamine-*N*-[amino(polyethylene glycol)-2000] (ammonium salt) (DSPE-PEG) and DSPE-PEG-folate (DSPE-PEG-FA) were purchased from Avanti Polar Lipids (China). All other materials are of reagent grade and used as such.

Synthesis of DOX/EDL-Loaded Lipid–Polymer Targeted Nanoparticles (DE-PLN or DE-FPLN)
The DOX/EDL-loaded lipid–polymer nanoparticles (DE-PLN) or DOX/EDL-loaded folate-conjugated lipid–polymer nanoparticles (DE-FPLN) were prepared by nanoprecipitation method. PLGA (10 mg), DOX (1 mg), and EDL (1 mg) were dissolved in acetonitrile and mixed together. Following this, lecithin and DSPE-PEG or DSPE-PEG-FA (4:1 molar ratio) were dissolved in 5% ethanol aqueous solution at a weight ratio of 20% to that of PLGA mixture. The lipid fraction is heated at 65 °C for 5 min. The PLGA/acetonitrile solution was gradually added to the lipid solution in a dropwise manner to allow the self-assembly process. The organic solvents were gradually removed at 37 °C via a rotary evaporation method. The thus-formed nanoparticle was washed thrice with distilled water using a centrifugal device with a molecular weight cutoff of 3500 kDa. The nanoparticle was suspended in distilled water and stored at 4–8 °C until further use. As much as possible, drug-loaded nanoparticles were prepared fresh for all the experiments. The drug-loaded nanoparticles were centrifuged and supernatant was collected to determine the unentrapped drug. The drug entrapment efficiency (EE) was calculated using %EE=[Drug added–Unentrapped drug)/Total drug added]×100 and drug loading efficiency (LE) was calculated using %LE=[Entrapped drug/Nanoparticles weight]×100. The size and size distribution of nanoparticles were determined at 25 °C using dynamic light scattering (DLS) (Zetasizer Nano-ZS; Malvern Instruments, UK) equipped with a 633 nm He–Ne laser using back-scattering detection. The experiments were performed in triplicate. The stability of nanoparticles over a period of 30 days was evaluated in terms of particle size. The nanoparticles maintained excellent stability with no significant change in particle size.

In Vitro Drug Release Study
The drug release of DOX and EDL from DE-FPLN was studied using a dialysis tube (Spectra/Pore, MWCO 3500). Freeze-dried DE-FPLN containing 1 mg equivalent of DOX or EDL was dissolved in 1 mL of respective buffers. The study was performed at 37 °C in a regular shaker (100 rpm). The dual drug-loaded nanoparticle dispersions were sealed in a dialysis tube and placed in a 30 mL of acetate buffered saline (ABS, pH 5.0) and phosphate buffered saline (PBS, pH 7.4) in a Falcon tube. The tube was placed in a shaker bath at a speed of 100 rpm/min and maintained at 37 °C. At a predetermined time, small aliquots of samples were collected and replaced with equal volume of the fresh sample to maintain the sink conditions. The amount of drug released in the buffer was calculated using HPLC method. The HPLC system (Waters, Milford, MA, USA) consists of a Waters 1525 Binary HPLC pump, a Waters 2707 Autosampler, and a Waters 2475 multi λ fluorescence detector. A C-18 column (150 mm×4.6 mm, 5 µm particle size, and 100 Å pore size; AkzoNobel/Kromasil, Brewster, NY, USA) was used at room temperature. Flow rate was maintained at 1 mL per minute.

In Vitro Cell Culture
MG63 osteosarcoma cells (ATCC, Manassas, VA, USA) were cultured in RPMI-1640 growth medium supplemented with 10% FBS and 1% antibiotic mixture. The cells were grown in ambient conditions of 5% carbon dioxide and moisture status.

In Vitro Cellular Uptake
The targeting ability of nanoparticles toward MG63 cells was studied by confocal laser scanning microscopy (CLSM). For this purpose, Nile Red-loaded PLN or FPLN was prepared by nanoprecipitation method. The DOX/EDL was replaced with hydrophobic Nile Red during the synthesis of nanoparticles as mentioned above. The individual wells in the 6-well plate were covered with a cover slip and $2×10^5$ cells per well were seeded and incubated for 12 h. Next day, cells were exposed with 100 µL of DE-PLN or DE-FPLN-loaded with fluorescent Nile Red at a concentration of 0.25 µg/mL and incubated for 2 h. The concentration of nanoparticles was 50 µg/mL. The cells were washed and fixed with 4% paraformaldehyde and

incubated for 10 min followed by staining with DAPI solution for 5 min. The cells were well rinsed with PBS and observed under a confocal microscope (Zeiss LSM 710; Carl Zeiss Meditec AG).

In Vitro Cytotoxicity Assay

The in vitro cytotoxicity assay in MG63 cancer cell was evaluated by MTS as per the guidelines of manufacturers of CellTiter 96® Aqueous One Solution Cell Proliferation Assay (Promega, Madrid, Spain). In brief, 8000 cells were seeded in the each well of a 96-well plate and incubated for 24 h. After that, cells were treated with free drugs or free drug cocktail or DE-PLN/DE-FPLN and incubated for 24 h. Then, 100 μg of lipid–polymer nanoparticles was used for the highest test concentration of DOX or EDL (10 μg/mL). After 24 h, supernatant and all media were removed and washed twice with PBS. The cells were then added with 100 μL of complete media containing 15 μL of MTS solution and incubated for 4 h. The absorbance was measured using a microplate reader (iEMS reader MF; Labsystem, Helsinki, Finland) at a wavelength of 690 nm. The cells were carefully washed 3 times using PBS to remove all the metabolites and nanoparticle residues to avoid any interference with the MTS dye. The untreated cells were used as a control and compared to treatment groups. The IC50 value calculations and statistical analysis was performed using GraphPad Prism software. The combination index was calculated using CalcuSyn software (Biosoft, Cambridge, UK). A CI value of less than 0.9 indicates synergism while 0.9–1.1 indicates additive and anything above 1.1 indicates the antagonistic characteristics.

Caspase-3/7 Activity

The caspase-3/7 activity was evaluated using a Caspase-Glo-3/7 assay kit (Promega, USA) as per the manufacturer's protocol. In brief, 8000 cells were seeded in each well of a 96-well plate and incubated for 24 h. After that, cells were treated with different concentrations of free drugs and free drug combination and drug-loaded nanoparticles, and incubated for 24 h. After 24 h, supernatant and all media were removed and washed twice with PBS. The caspase activity was measured by adding the assay reagent in a proportion of 1:1 to each well. The luminescence signal was measured using a Tecan GENios microplate reader (Tecan Group Ltd, Switzerland) after incubating for 30 min post reagent addition. The experiments were performed in triplicate.

Pharmacokinetic Analysis of DE-FPLN

Sprague-Dawley rats (male) weighing 200±10 g were divided into four groups of 5 rats (DOX, EDL, DE-FPLN (DOX), and DE-FPLN (EDL)). The animals were caged in an animal house maintained at 25 °C and 60% RH. All the animal studies are performed in compliance with the Institutional Animal Ethical Care and Management (IAECM) guidelines, Luoyang Orthopedic Hospital of Henan Province, China. The protocol was approved by the Animal Ethics Committee of Luoyang Orthopedic Hospital of Henan Province. The animals were housed and cared for in accordance with the Guide for the Care and Use of Laboratory Animals (eighth edition). The animals were received free DOX, free EDL, and DE-FPLN (DOX/EDL) by intravenous administration at a fixed dose of 5 mg/kg. Free DOX and EDL were dissolved in PEG 400 and administered at a dose of 5 mg/kg. In the case of DE-FPLN, the lyophilized powder was dissolved in physiological saline (0.9% NaCl). Blood samples (300 μL) were collected from the right femoral artery at pre-determined times (15 min, 30 min, 1 h, 2 h, 4 h, 8 h, 12 h, and 24 h, respectively) after administration of these formulations. The samples were collected in heparin-containing tubes (100 IU/mL) and then immediately centrifuged (Eppendorf, Hauppauge, NY, USA) at 12,000 rpm for 10 min. The plasma supernatant was collected and stored at −20 °C until further analysis. The DOX/EDL was extracted after the precipitation of unwanted protein. Then, 150 μL of plasma was mixed with 150 μL of acetonitrile for 30 min. The samples were then centrifuged at 12,000 rpm for 10 min and 10 μL of the supernatant was injected into the HPLC system for DOX and EDL analysis.

In Vivo Antitumor Efficacy

The BALB/c female mice with an average weight ranging from 20 to 22 g were purchased and given humane care with free access to food and water. All the animal studies are performed in compliance with the Institutional Animal Ethical Care and Management (IAECM) guidelines, The Eighth People's Hospital of Shanghai, China. In brief, MG63 cells were grown in the culture medium and after 80% confluence the cells were harvested from the culture flask and subcutaneously implanted in the right flank of the mice in the capacity of 5×10^6 cells/mouse. The tumor growth was closely observed and the experiment was initiated when the tumor volume reaches approximately 100 mm³. The mice were divided into 6 groups with 8 mice in each group. The mice groups were administrated

with free DOX, EDL, DOX/EDL cocktail, DE-PLN, and DE-FPLN at a maximum dose of 5 mg/kg of mice body weight 3 times on days 1, 4, and 7. The total duration of each experiment was 20 days and a total of 48 mice were used for the study. All mice were tagged and tumor volumes were measured at a predetermined time interval using the tumor volume (V) calculation formula $V=a \times b \times 1/2$, where "a" and "b" are respectively long and short diameters of the tumor. The tumor size was measured using a vernier caliper.

Histological Analysis of Tumors

The tumors were surgically removed from the mice after sacrificing them humanely following all the animal handling protocols. The extracted tumors were fixed in 10% formalin for 2 h and then embedded in paraffin at a thickness of 5 mm. The tissue section is then subjected to H&E staining and observed through the fluorescence microscope (Olympus, NIKON).

Statistical Analysis

All data are presented as the mean±standard deviation. All statistical analysis was performed using SPSS 10.0 software (SPSS Inc., Chicago, IL, USA). A statistical difference of $p<0.05$ was considered significant.

Results and Discussion
Formulation and Optimization of DOX/EDL-Loaded Folate-Targeted Lipid–Polymer Nanoparticles

The schematic presentation of preparation of DOX/EDL-loaded lipid–polymer hybrid nanoparticles is presented in Figure 1. The DOX and EDL along with PLGA were dissolved in organic solvent and stirred. The lipid mixture was added to the polymeric solution and allowed to form the self-assembly, resulting in the creation of lipid–polymer hybrid nanoparticles. The hydrophobic nature of the drugs allowed stable incorporation in the lipid matrix and hydrophobic PLGA. Earlier, studies have shown that the presence of PEG on the outer surface will ensure protection from the reticuloendothelial (RES)-based clearance system that could potentially result in the prolonged blood circulation and reduced non-specific binding. The presence of folic acid moiety will confer the targeting capacity to the nanoparticles toward the tumors tissues in the body.

The particle size and surface charge characteristics were evaluated by dynamic light scattering (DLS) analysis. The mean particle size of DE-FPLN was observed to be 122.5 ±2.45 nm with a narrow distribution index of 0.140 (Figure 2A). The average surface charge of DE-FPLN was observed to be −18.4±1.26 mV. The particle size was further confirmed by the TEM imaging (Figure 2B). All the particles were perfectly spherical in shape and uniformly spread over the copper grid. Especially, a grayish shell was observed at the periphery of each particle that might be due to the presence of a lipid shell. A particle in the nanosize range is deemed suitable for the tumor targeting as it can penetrate the tumor tissues via enhanced permeation and retention (EPR) property. It is reported and widely recognized that tumors possess leaky vasculature coupled with poor drainage access, which allows the high accumulation of particles and intracellular concentrations when the particles are nanosized.[22] The loading capacity of DOX in DE-FPLN was 6.89% w/w while EDL was 5.75% w/w, respectively.

In Vitro Drug Release

The release of DOX and EDL from DE-FPLN under different pH conditions was evaluated by dialysis method. As
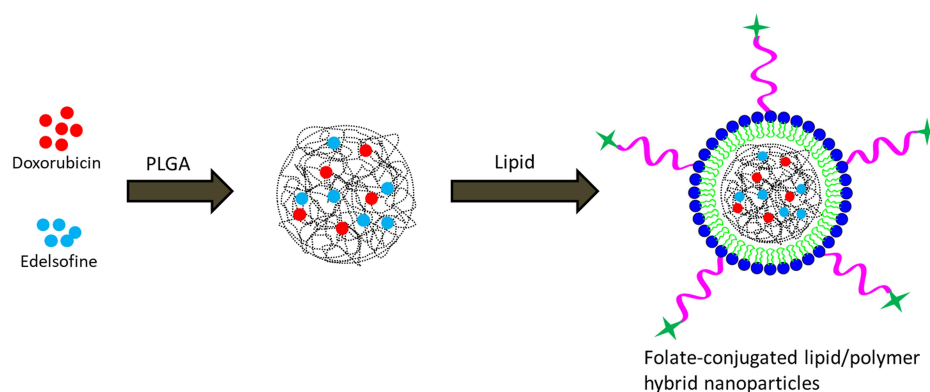

Figure 1 Schematic illustration of formulation design. Schematic presentation of preparation of DOX and EDL-loaded folic acid targeted lipid–polymer hybrid nanoparticles.
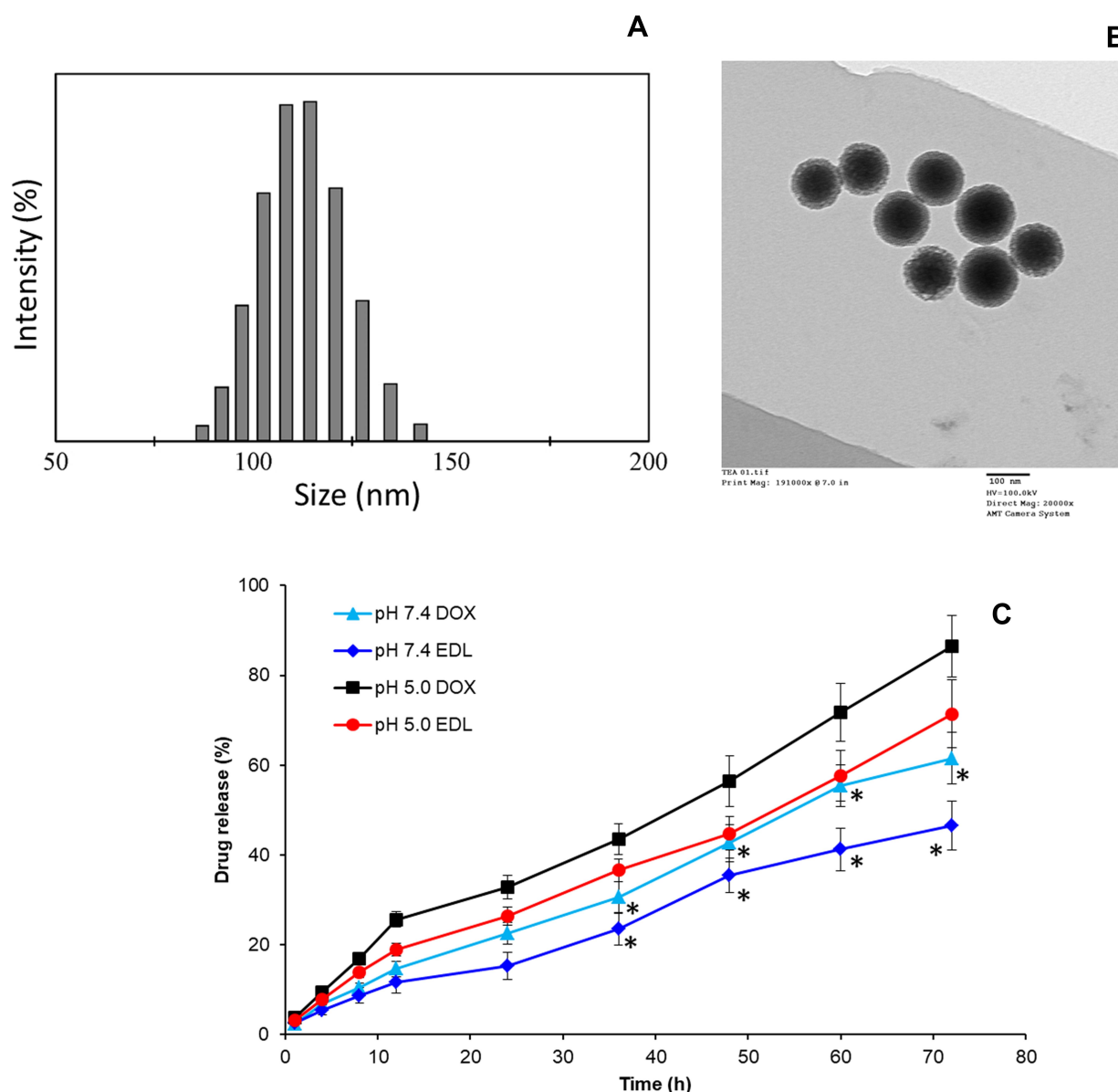
Figure 2 Physicochemical characterization of nanoparticles. (**A**) Particle size distribution of DE-FPLN by dynamic light scattering (DLS) analysis; (**B**) particle morphology analysis by transmission electron microscopy (TEM); (**C**) in vitro drug release profile of DOX and EDL from DE-FPLN nanoparticles. The drug release study was performed by dialysis method in phosphate buffered saline (pH 7.4) and acetate buffered saline (pH 5.0). The drug release amount was quantified by HPLC method. *$p<0.05$ is the statistical difference between different conditions. Data are presented as mean±SD (n=3 per group).

seen (Figure 2C), a differential release pattern was observed under physiological and acidic pH conditions. The release rate of drugs was higher in acidic conditions compared to that in pH 7.4 conditions. For example, ~18% of DOX was released in 24 h in pH 7.4 conditions compared to ~32% in pH 5.0 conditions. Similarly, 12% of EDL was released in 24 h in pH 7.4 conditions compared to nearly 25% EDL release in pH 5.0 conditions. It should also be noted that the release rate of DOX was relatively higher than that of the release rate of EDL in both pH conditions.

A differential release pattern for both the drugs might be attributed to the encapsulation of one drug in the polymer core and another in the lipid matrix or vice versa. Importantly, both the drugs showed a sustained release of drug from the nanoparticles. The release trend continued until the end of the study period with higher release in acidic media mimicking the tumor microenvironment. This type of sequential release of drugs in the tumor cells results in effective synergistic therapeutic effects. Besides, enhanced drug release in lower pH conditions compared to that in

physiological conditions boosts the prospect of higher drug release in the lysosomal/endosomal pH conditions in the tumors.[26]

destabilized and result in the release of encapsulated drugs. These drugs then reach their targeted location inside the tumors.

Intracellular Uptake in MG63 Osteosarcoma Cells

The targeting ability of the nanoparticles (DE-PLN and DE-FPLN) in MG63 cancer cells was evaluated by confocal laser scanning microscopy (Figure 3). CLSM images showed a red fluorescence from Nile Red-loaded nanoparticles in the lysosomal regions of cancer cells. Data clearly reveal that folic acid-targeted nanoparticle (DE-FPLN) showed a remarkably stronger red fluorescence compared to that of non-targeted DE-PLN, indicating that the receptor-mediated internalization via FR-mediated endocytosis might be responsible for enhanced accumulation of particles. FR targeting played a seemingly crucial role in enhancing the cellular uptake of nanoparticles by MG63 cells. Accumulation of non-targeted nanoparticles in the cancer cells further highlights the fact that other mechanisms such as clathrin or caveolae-mediated could be associated with the nanoparticle uptake. It is believed that nanoparticles enter the acidic lysosomes and the nanoparticles get

In Vitro Cell Viability – Combination Index

Administration of single drugs often resulted in poor efficacy and multidrug resistance (MDR). In this regard, combination chemotherapy has been proven to be remarkably effective compared with single drugs. The use of multiple drugs will act on the different pharmacological pathways and prevent the drug resistance and improve the therapeutic efficacy. It is well known that a specific ratio of drugs is particularly more effective while certain ratios are ineffective. In order to evaluate the perfect ratio of two drugs, drugs were combined in different ratiometric combination and cell viability was evaluated. As seen (Figure 4A), different ratiometric combinations have different effects on the cell viability of cancer cells. The therapeutic effect of combinations of drugs are evaluated in terms of synergistic, additive, and antagonistic. The Chou and Talalay method-based CI tells that the values below <0.9 indicate drug synergy while CI between 0.9 and 1.1 indicates additive nature and >1.1 indicates the antagonistic effect of the drugs. As seen,
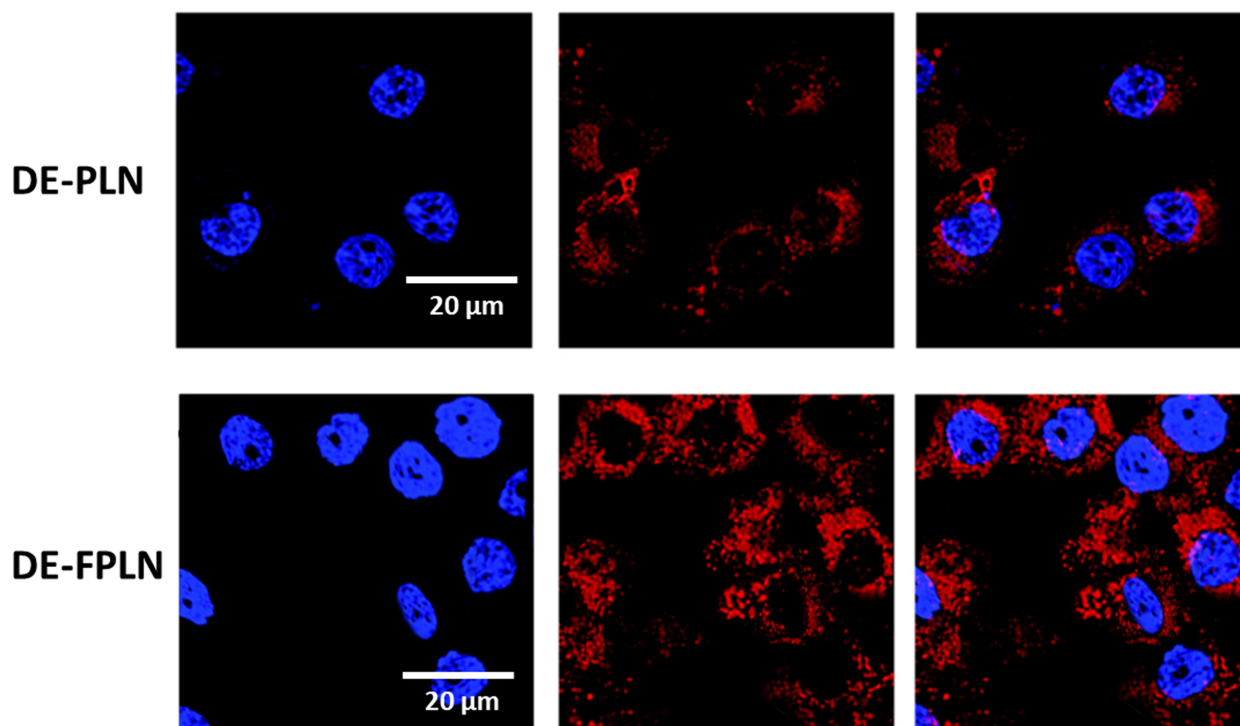

Figure 3 Cellular uptake analysis in oteosarcoma. In vitro cellular uptake study in MG63 cancer cells. The distribution of DE-PLN and DE-FPLN in MG63 cancer cells was evaluated by confocal laser scanning microscopy using Nile Red as a fluorescent moiety.
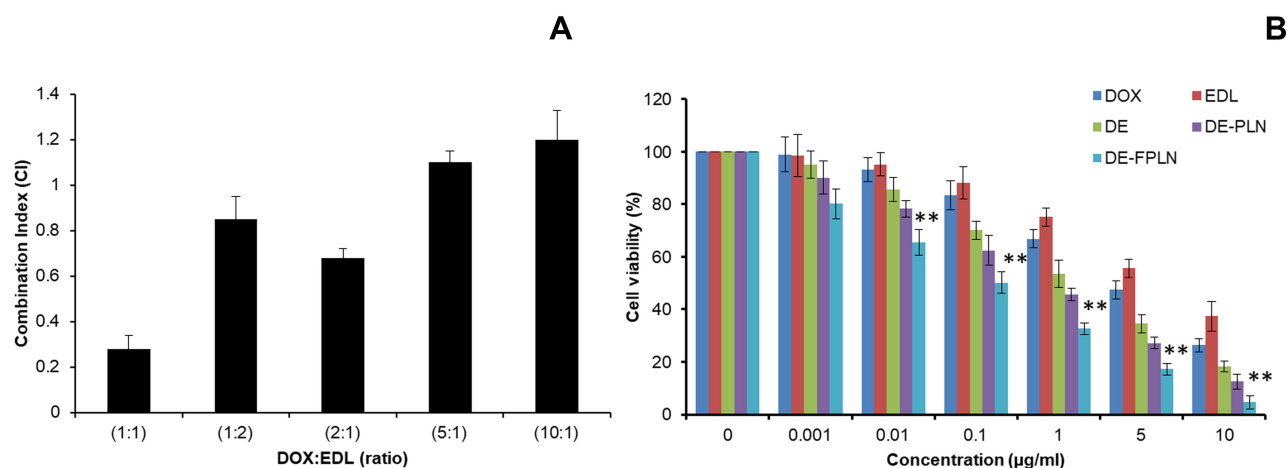
Figure 4 In vitro anticancer effect of drug combination. (**A**) Combination index analysis of different ratiometric combinations of DOX and EDL. The cell viability was determined and then fitted in Calcusyn software. Data are presented as mean±SD (n=3 per group). (**B**) Cell viability analysis using MTS assay. A fixed ratio of 1:1 of DOX: EDL was used to load in the nanoparticles. **$p<0.001$ is the statistical difference between free DOX and DE-FPLN. Data are presented as mean±SD (n=6 per group).

DOX:EDL were highly synergistic in 1:1 w/w ratio, indicating a maximal synergistic interaction between the drugs. The DOX:EDL at 1:2 and 2:1, although synergistic, were less compared to that of 1:1 ratiometric combinations. On the contrary, drug ratios of 5:1 and 10:1 were antagonistic in nature. Based on the C1 value, we have chosen DOX:EDL to study further for all the in vitro and in vivo studies.

In Vitro Cytotoxicity Assay

Following the ratiometric analysis of DOX and EDL, the in vitro cytotoxic effect of free drugs and drug-loaded nanoparticles (targeted and non-targeted) was evaluated in MG63 osteosarcoma cells. As seen (Figure 4B), all the formulations showed a typical dose-dependent cytotoxic effect in the cancer cells. The cell viability of cocktail DOX:EDL (DE) treated cells was significantly lesser compared to that of single drugs, either DOX or EDL alone, further suggesting the potential of combination of drugs. It should be noted that dual drug-loaded nanoparticles showed relatively higher anticancer effect than the free combination of drugs. Importantly, folate receptor-targeted DE-FPLN showed a remarkable anticancer effect in the MG63 cancer cells. The cytotoxicity profiles were fitted in a logistic model to calculate the IC50 value – a concentration required to kill 50% of the cancer cells. The IC50 values of DOX, EDL, DE, DE-PLN, and DE-FPLN stood at 4.5 µg/mL, 6.4 µg/mL, 2.3 µg/mL, 1.08 µg/mL, and 0.26 µg/mL, respectively. Data clearly reveal the superior anticancer potential of DE-FPLN formulation in controlling the proliferations of cancer cells. Although DE-PLN showed notable decrease in cell viability due to the combination therapeutics, DE-FPLN

showed the significantly lower cell viability attributed to the higher cellular internalization of targeting a ligand-based carrier system.

We have performed the additional cell viability assay on normal human normal osteoblast cells (NHOC) (Figure S1). As shown, free drugs as well as drug-loaded formulations killed the NHOC cells in a concentration-dependent manner. There is no statistical difference between the cell killing effect between NHOC and MG63 cells. However, one of the importance differences between NHOC and MG63 cells is that cell viability of DE-FPLN was not statistically different from that of DE-PLN due to lack of overexpressed folate receptors in normal cells. It must be understood, however, that DE-FPLN exhibits the cytotoxic effect in the normal cells in the in vitro conditions. In the systemic circulation, long circulation ability of DE-FPLN will allow the preferential accumulation in the cancer cells and minimize its uptake in the normal cells, and thereby minimize the adverse effect.[27–29]

Caspase-3/7-Based Apoptosis Activity

The mechanism of cell death was evaluated in terms of cell apoptosis using caspase-3/7 activity assay in MG63 cells. For this purpose, MG63 cells were exposed with different formulations and incubated for 24 h. As seen (Figure 5A), caspase-3/7 activity of cocktail DE remarkably increased compared to that of single drug treatment. Consistent with the cell viability assay, DE-PLN showed higher caspase-3/7 activity than that of free drug cocktails. Interestingly, DE-FPLN showed 1.5-fold and 3-fold higher caspase-3/7 activity compared to that of DE-PLN and DE cocktail, indicating that the co-administration of two drugs in a folic
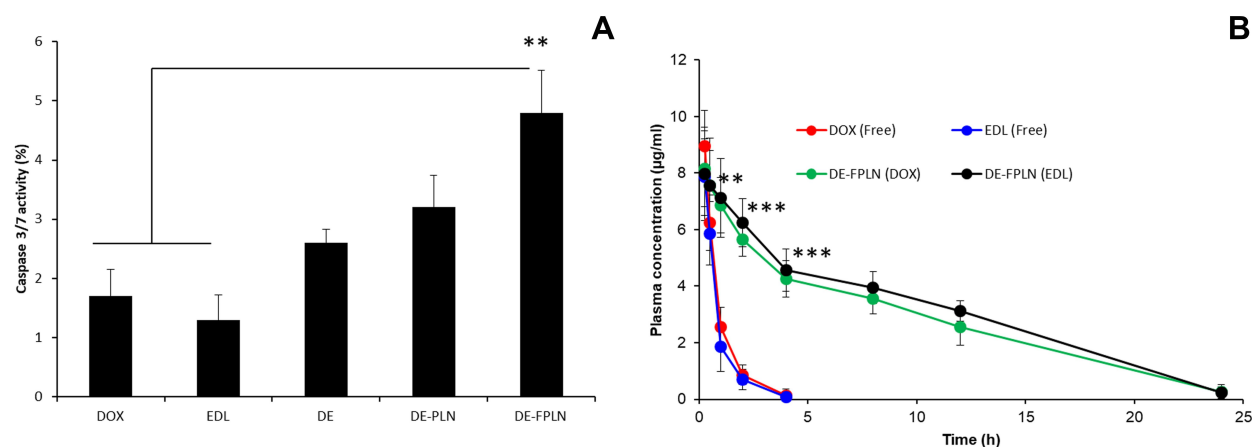
Figure 5 Apoptosis and pharmacokinetic analysis. (**A**) Caspase-3/7 activity analysis was performed by Caspase-Glo 3/7 luminescence assay after incubation for 24 h. Different formulations of single and dual-drug were treated with MG63 cancer cells. (**B**) Pharmacokinetic analysis of free DOX/EDL and DE-FPLN in animals. The formulations were administered intravenously and blood was collected in a timely manner. **$p<0.001$ and ***$p<0.0001$ is the statistical difference between free DOX and DE-FPLN.

acid-targeted nanoparticle could potentially induce the apoptosis and cell death. Such enhancing of cytotoxic activity between DOX and EDL has been reported in Ewing's sarcoma cells and could be attributable due to different mechanisms of actions.[30] DOX is reported to exert its pharmacological effect by the inhibition of DNA synthesis in the nucleus while EDL targets the cell membrane, mitochondria, and endoplasmic reticulum.[31,32]

Pharmacokinetic Analysis

The plasma concentration–time profiles of DOX and EDL following single dose intravenous (IV) administration of free form and nanoparticle encapsulated form are presented in Figure 5B. Free DOX, EDL, and DE-FPLN (DOX/EDL) were administered at a dose of 5 mg/kg via the femoral vein. Free DOX and EDL were rapidly cleared from the circulation within 4 h of IV administration and exhibited linear pharmacokinetics. As reported previously, the linear pharmacokinetic profile of DOX remained the same whether administered at high or low dose. In contrast, DOX and EDL had a remarkably prolonged plasma circulation time after administration of DE-FPLN (DOX/EDL) and maintained a therapeutic drug level throughout the study period. For example, 0.121 ± 0.25 μg/mL of free DOX was observed after 4 h of IV administration whereas 0.256 ± 0.21 μg/mL of DOX was observed from nanoparticle formulation after 24 h, indicating the superior potential of a carrier-mediated delivery system. The prolonged blood circulation profile of DE-FPLN was mainly attributed to the shielding effect of PEG, the excellent stability of the carrier/drug formulation in

blood circulation, and the negative surface charge of the nanoparticles. Additionally, nanosized particles might be able to evade the macrophage system in the systemic blood circulation. The presence of a PEG outer shell in the micelles reduced the effective surface charge and increased the hydrophilicity that would decrease the liver and splenic uptake.

In Vivo Antitumor Efficacy

The therapeutic efficacy of formulations was evaluated by the intravenous administration for formulations in the tumor-bearing mice model. The mice were administered with DOX, EDL, DE, DE-PLN, and DE-FPLN, respectively. As shown (Figure 6A), free DOX and EDL did not have much effect on the tumor growth while cocktail combination DE showed obvious tumor regression compared to single treatment and control. Importantly, DE-FPLN outperformed all the other groups and significantly delayed the tumor progression in the animal models. DE-FPLN showed 1.5-fold lower tumor volume than DE-PLN while it showed 2-fold lower tumor volume and 3-fold lower tumor volume for DE and single drugs, respectively. The main reason behind the excellent antitumor efficacy might be due to prolonged blood circulation and active targeting of the nanoparticles to the tumor tissues.[33] The folate receptors overexpressed in the tumors will bind specifically to the folic acid ligand conjugated on the nanoparticle surface and results in enhanced accumulation in the local area and high therapeutic efficacy. Significant differences in tumor volume were observed between mice treated with 2.5 mg/kg and 5 mg/kg; however,
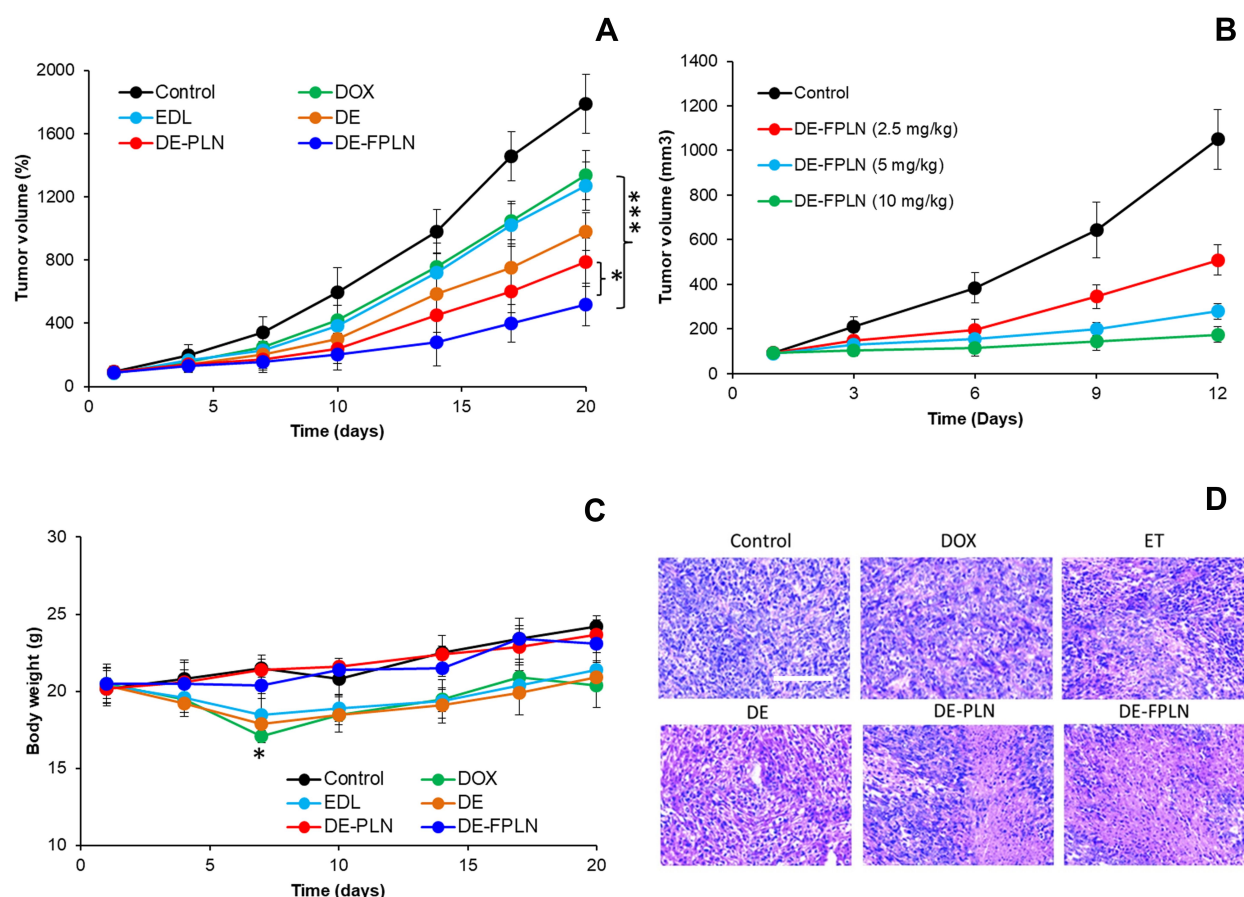
Figure 6 In vivo therapeutic efficacy analysis of combinational nanoparticles. (**A**) In vivo antitumor efficacy analysis in the MG63 cancer cell-bearing xenograft model. The tumor mice were administered with doxorubicin (DOX), edelfosine (EDL), doxorubicin and edelfosine cocktail (DE), DOX/EDL-loaded polymer–lipid nanoparticles (DE-PLN), and DOX/EDL-loaded folate-conjugated polymer–lipid nanoparticles (DE-FPLN) and the tumor volumes were measured by vernier caliper. The free drug and formulations were administered at a dose of 5 mg/kg. (**B**) Tumor volume measurement following the different dose administration of DE-FPLN (2.5, 5, and 10 mg/kg). (**C**) Body weight analysis as a marker for toxicity patterns. The free drug and formulations were administered at a dose of 5 mg/kg. (**D**) H&E analysis of tumors extracted from different animal groups. The mice were sacrificed and tumors were extracted and subjected to H&E analysis. *$p<0.05$ and ***$p<0.001$ is the statistical difference between the indicated groups. Scale bar is 100 µm.

insignificant difference was observed at higher doses (Figure 6B). Except at the last time point, mice treated with 5 mg/kg and 10 mg/kg were insignificant. The experiment further reiterates the fact that 5 mg/kg of the combination of DOX and EDL could be appropriate. Besides, hallmarks of tumors are characterized by the presence of poor lymphatic drainage and leaky vasculature that allows the internalization of nanocarriers sized up to ∼200 nm specifically into the tumoral regions, commonly referred to as the EPR effect. The features of improved physiological stability and prolonged blood circulation contributed to selective accumulation and long-term retention of DE-FPLN at the tumor sites and enhanced therapeutic efficacy. González-Fernández et al have reported a synergistic effect of DOX and EDL. The authors reported that the synergistic effect was well-correlated with caspase-3/7 activity indicating a caspase-mediated cell death.[34] Other

authors also observed the combination effect of DOX and EDL in Ewing's sarcoma cells.[31] DOX is known to exert its effect by inhibition of DNA synthesis in the nucleus, while EDL targets the membrane of the cells, endoplasmic reticulum, and mitochondria. Stability and suitability of carriers also played an important role in enhancing the anticancer effect of encapsulated drugs. For example, Zhang et al reported the enhanced anticancer effect employing similar polymer–lipid hybrid nanoparticles.[35] The authors have reported that polymer–lipid hybrid nanoparticles improved the pharmacokinetic profile of dual drugs (DOX and Mitomycin C) and enhanced the antitumor effect in xenograft breast cancers.

H&E analysis revealed that DE-FPLN exerted remarkable damage to the tumor tissues compared to any other administered groups (Figure 6C). DE-FPLN-treated tumors exhibited pyknotic cells in which nuclei were condensed,

which are seemingly signs of apoptosis and dead cells. Furthermore, mice treated with DE-FPLN did not show any significant changes in the body weight throughout the study period, indicating a lack of any toxic effects. In contrast, mice treated with free DOX and DE resulted in 10% shedding of body weight, which is consistent with the other reports of toxicity (Figure 6D). In the case of DE-FPLN, a low dosage of both drugs which is stably incorporated in the nanoparticles was beneficial in reducing the side effects and highlights the superior advantages of the nanocarrier system. The significant improvement in the antitumor efficacy stems from the fact that DE-FPLN delivers the drug to the tumor tissues in a specific ratiometric manner that allows the synergistic killing of the cancer cells and tumor regression. In contrast, free drug and cocktail combinations (DE) may not equally penetrate the tumors and result in subpar therapeutic effect.

Acute Toxicity Analysis

Drug-related toxicity to major organs was evaluated by H&E staining. Free DOX treatment to the animals resulted in serious damage to the liver, kidney, and heart (Figure 7). EDL was relatively less toxic compared to that of DOX as observed from the H&E image. Hepatic lesions were observed with severe atrophy of hepatic cells. The free DOX resulted in acute cellular swellings of the liver and the mean hepatocyte diameter for the free DOX-treated group was 26.18 ± 2.16 μm compared to 14.25 ± 1.68 μm in the non-treated animal group. Cardiac H&E revealed that free DOX resulted in focal rarefactions, focal areas of disrupted cardiac muscle fibers, and cytoplasmic vacuolization. In contrast, DE-FPLN showed no myocardial degeneration and was devoid of any cardiotoxicity. The kidney in the DE and DOX-treated group showed notable
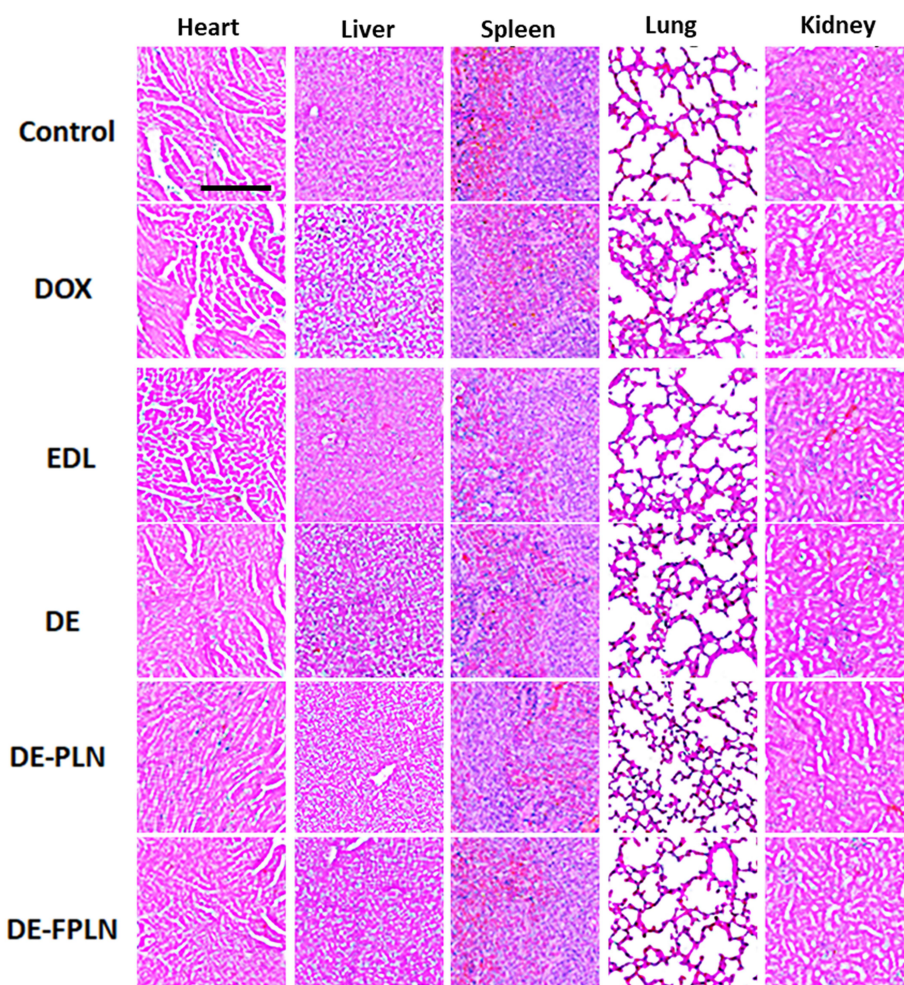

Figure 7 In vivo toxicity analysis in the animal model. Acute toxicity analysis of free drugs and drug-loaded formulations in vital organs included the heart, liver, spleen, lungs, and kidney by H&E staining analysis. The toxicity of DOX in the heart is highlighted by arrow marks which showed disrupted cardiac muscle fibres and cytoplasmic vacuolization. Liver and kidney of the DOX-treated group showed signs of marked degenerative changes. Scale bar is 100 μm.

congestion with marked degenerative changes, and disrupted epithelium. The sections of liver in the DE and DOX-treated group showed marked central vein congestion, marked bile duct hyperplasia, and dilation of sinusoidal spaces, and some sections showed marked degenerative changes. The H&E stained sections of liver and kidney from the formulation-treated group appeared normal, suggesting lack of any hepatotoxicity or nephrotoxicity. No such damage or sign of toxicity was observed in DE-FPLN-treated animal group, suggesting the efficacy of carrier-based drug delivery. The ability of the carrier system to decrease the organ damage and increase the anticancer efficacy is of great significance.

Despite the excellent findings in this investigation, the study is not without limitations. It was assumed in this study that a higher dose would confer greatest efficacy; however, in terms of toxicity, the maximum tolerable dose (MTD) is not determined. The acute toxicity effect monitoring performed in the current study was done only at the dose range tested, but not at the MTD of the various compounds involved (as the MTDs have not been determined). Future studies will focus on quantifying dose–response effects, with simultaneous emphasis on MTD. Furthermore, we would like to continue the study with different targeting ligands or combination of two or more ligands.

Conclusions

In conclusion, we have prepared a novel folate receptor-targeted doxorubicin and edelfosine-loaded lipid–polymer hybrid nanoparticle to enhance the anticancer efficacy in osteosarcoma. The targeted nanoparticles showed enhanced cellular internalization and subcellular distribution in MG63 cancer cells compared to that of non-targeted nanoparticles. MTT assay and caspase-3/7 activity assay clearly showed the superior anticancer efficacy of DE-FPLN formulations in inducing cancer cell death. In vitro results indicate that the co-administration of two drugs in a folic acid-targeted nanoparticle could potentially induce the apoptosis and cell death. In vivo results displayed the potency of tumor cell killing and significant suppression of tumor growth without any detectable side effects. The lipid–polymer hybrid nanocarriers with multiple properties of high drug loading, sequential and ratiometric drug release, improved physiological stability, prolonged blood circulation, and tumor-specific targeting are promising for the delivery of multiple drugs in the treatment of osteosarcoma.

Disclosure

The authors report no conflicts of interest for this work.

References

1. Kansara M, Teng MW, Smyth MJ, Thomas DM. Translational biology of osteosarcoma. *Nat Rev Cancer*. 2014;14(11):722–735. doi:10.1038/nrc3838
2. Botter SM, Neri D, Fuchs B. Recent advances in osteosarcoma. *Curr Opin Pharmacol*. 2014;16:15–23. doi:10.1016/j.coph.2014.02.002
3. Ferrari S, Smeland M, Mercuri F, et al. Neoadjuvant chemotherapy with high-dose ifosfamide, high-dose. methotrexate, cisplatin, and doxorubicin for patients with localized osteosarcoma of the extremity: a joint study by the Italian and Scandinavian Sarcoma Groups. *J Clin Oncol*. 2005;23(34):8845–8852. doi:10.1200/JCO.2004.00.5785
4. Schwartz CL, Gorlick R, Teot L, et al. Multiple drug resistance in osteogenic sarcoma: INT0133 from the Children's Oncology Group. *J Clin Oncol*. 2007;25(15):2057–2062. doi:10.1200/JCO.2006.07.7776
5. Siegel R, Naishadham D, Jemal A. Cancer statistics, 2013. *CA Cancer J Clin*. 2013;63(1):11–30. doi:10.3322/caac.21166
6. Ramasamy T, Ruttala HB, Sundaramoorthy P, et al. Multimodal selenium nanoshell-capped Au@ mSiO 2 nanoplatform for NIR-responsive chemo-photothermal therapy against metastatic breast cancer. *NPG Asia Mater*. 2018;10(4):197–216. doi:10.1038/s41427-018-0034-5
7. Tran TH, Ramasamy T, Choi JY, et al. Tumor-targeting, pH-sensitive nanoparticles for docetaxel delivery to drug-resistant cancer cells. *Int J Nanomedicine*. 2015;10:5249–5262. doi:10.2147/IJN.S89584
8. Thorn CF, Oshiro C, Marsh S, et al. Doxorubicin pathways: pharmacodynamics and adverse effects. *Pharmacogenet Genomics*. 2011;21(7):440–446. doi:10.1097/FPC.0b013e32833ffb56
9. Bonilla X, Dakir E, Mollinedo F, Gajate C. Endoplasmic reticulum targeting in Ewing's sarcoma by the alkylphospholipid analog Edelfosine. *Oncotarget*. 2015;6(16):14596–14613.
10. Yao C, Wei JJ, Wang ZY, et al. Perifosine induces cell apoptosis in human osteosarcoma cells: new implication for osteosarcoma therapy? *Cell Biochem Biophys*. 2013;65:217–227. doi:10.1007/s12013-012-9423-5
11. Gonz alez-Fernandez Y, Zalacain M, Imbuluzqueta E, Sierrasesumaga L, Patino-García A, Blanco-Prieto M. Lipid nanoparticles enhance the efficacy of chemotherapy in primary and metastatic human osteosarcoma cells. *J Drug Deliv Sci Technol*. 2015;30:435–442.
12. Estella-hermoso de Mendoza A, Preat V, Mollinedo F, Blanco-Prieto MJ. In vitro and in vivo efficacy of edelfosine-loaded lipid nanoparticles against glioma. *J Control Release*. 2011;156(3):421–426. doi:10.1016/j.jconrel.2011.07.030
13. Mollinedo F, Fernandez-Luna JL, Gajate C, Martin-Martin B, Benito A, Martinez-Dalmau R. Selective induction of apoptosis in cancer cells by the ether lipid ET-18-OCH3 (Edelfosine): molecular structure requirements, cellular uptake, and protection by Bcl-2 and Bcl-X(L). *Cancer Res*. 1997;57:1320–1328.
14. Gajate C, Mollinedo F. Biological activities, mechanisms of action and biomedical prospect of the antitumor ether phospholipid ET-18-OCH(3) (edelfosine), a proapoptotic agent in tumor cells. *Curr Drug Metab*. 2002;3(5):491–525. doi:10.2174/1389200023337225

15. Ramasamy T, Ruttala HB, Gupta B, et al. Smart chemistry-based nanosized drug delivery systems for systemic applications: a comprehensive review. *J Control Release*. 2017;258:226–253. doi:10.1016/j.jconrel.2017.04.043

16. Hadinoto K, Sundaresan A, Cheow WS. Lipid-polymer hybrid nanoparticles as a new generation therapeutic delivery platform: a review. *Eur J Pharm Biopharm*. 2013;85:427–443. doi:10.1016/j.ejpb.2013.07.002

17. Li Y, Wu H, Yang X, et al. Mitomycin C-soybean phosphatidylcholine complex-loaded self-assembled PEG-lipid-PLA hybrid nanoparticles for targeted drug delivery and dual-controlled drug release. *Mol Pharm*. 2014;11:2915–2927. doi:10.1021/mp500254j

18. Ramasamy T, Ruttala HB, Chitrapriya N, et al. Engineering of cell microenvironment-responsive polypeptide nanovehicle co-encapsulating a synergistic combination of small molecules for effective chemotherapy in solid tumors. *Acta Biomater*. 2017;48:131–143. doi:10.1016/j.actbio.2016.10.034

19. Thevenot J, Troutier AL, David L, Delair T, Ladavière C. Steric stabilization of lipid/polymer particle assemblies by poly(ethylene glycol)-lipids. *Biomacromolecules*. 2007;8(11):3651–3660. doi:10.1021/bm700753q

20. Salvador-Morales C, Zhang L, Langer R, Farokhzad OC. Immunocompatibility properties of lipid-polymer hybrid nanoparticles with heterogeneous surface functional groups. *Biomaterials*. 2009;30(12):2231–2240. doi:10.1016/j.biomaterials.2009.01.005

21. Ai JW, Liu B, Liu WD. Folic acid-tagged titanium dioxide nanoparticles for enhanced anticancer effect in osteosarcoma cells. *Mater Sci Eng C Mater Biol Appl*. 2017;76:1181–1187. doi:10.1016/j.msec.2017.03.027

22. Montazerabadi A, Beik J, Irajirad R, et al. Folate-modified and curcumin-loaded dendritic magnetite nanocarriers for the targeted thermo-chemotherapy of cancer cells. *Artif Cells Nanomed Biotechnol*. 2019;47(1):330–340. doi:10.1080/21691401.2018.1557670

23. Kesharwani SS, Kaur S, Tummala H, Sangamwar AT. Overcoming multiple drug resistance in cancer using polymeric micelles. *Expert Opin Drug Deliv*. 2018;15(11):1127–1142. doi:10.1080/17425247.2018.1537261

24. Gottesman MM, Fojo T, Bates SE. Multidrug resistance in cancer: role of ATP-dependent transporters. *Nat Rev Cancer*. 2002;2(1):48–58. doi:10.1038/nrc706

25. González-Fernández Y, Brown HK, Patiño-García A, Heymann D, Blanco-Prieto MJ. Oral administration of edelfosine encapsulated lipid nanoparticles causes regression of lung metastases in pre-clinical models of osteosarcoma. *Cancer Lett*. 2018;430:193–200. doi:10.1016/j.canlet.2018.05.030

26. Brannon-Peppas L, Blanchette JO. Nanoparticle and targeted systems for cancer therapy. *Adv Drug Deliv Rev*. 2004;56:1649–1659. doi:10.1016/j.addr.2004.02.014

27. Sundaramoorthy P, Ramasamy T, Mishra SK, et al. Engineering of caveolae-specific self-micellizing anticancer lipid nanoparticles to enhance the chemotherapeutic efficacy of oxaliplatin in colorectal cancer cells. *Acta Biomater*. 2016;42:220–231. doi:10.1016/j.actbio.2016.07.006

28. Kanwar JR, A C R, Kanwar KA, Ganesh Mahidhara A, Cheung CHA. Cancer targeted nanoparticles specifically induce apoptosis in cancer cells and spare normal cells. *Australian J Chem*. 2012;65(1):5–14. doi:10.1071/CH11372

29. Wang J, Fang X, Liang W. Pegylated phospholipid micelles induce endoplasmic reticulum-dependent apoptosis of cancer cells but not normal cells. *ACS Nano*. 2012;6(6):5018–5030. doi:10.1021/nn300571c

30. Meng F, Cheng R, Deng C, Zhong Z. Intracellular drug release nanosystems. *Mater Today*. 2012;15(10):436–442. doi:10.1016/S1369-7021(12)70195-5

31. Bonilla X, Dakir E, Mollinedo F, Gajate C. Endoplasmic reticulum targeting in Ewing's sarcoma by the alkylphospholipid analog Edelfosine. *Oncotarget*. 2015;6(16):14596–14613.

32. Gajate C, Mollinedo F. Lipid rafts, endoplasmic reticulum and mitochondria in the antitumor action of the alkylphospholipid analog Edelfosine. *Anticancer Agents Med Chem*. 2014;14(4):509–527. doi:10.2174/1871520614666140309222259

33. Kesharwani SS, Kaur S, Tummala H, Sangamwar AT. Multifunctional approaches utilizing polymeric micelles to circumvent multidrug resistant tumors. *Colloids Surf B Biointerfaces*. 2019;173:581-590. doi:10.1016/j.colsurfb.2018.10.022

34. González-Fernández Y, Imbuluzqueta E, Zalacain M, Mollinedo F, Patiño-García A, Blanco-Prieto MJ. Doxorubicin and edelfosine lipid nanoparticles are effective acting synergistically against drug-resistant osteosarcoma cancer cells. *Cancer Lett*. 2017;388:262–268. doi:10.1016/j.canlet.2016.12.012

35. Zhang RX, Cai P, Zhang T, et al. Polymer-lipid hybrid nanoparticles synchronize pharmacokinetics of co-encapsulated doxorubicin-mitomycin C and enable their spatiotemporal co-delivery and local bioavailability in breast tumor. *Nanomedicine*. 2016;12(5):1279–1290. doi:10.1016/j.nano.2015.12.383